

Robo-AO: Initial results from the first autonomous laser guide star adaptive optics instrument

R. Riddle¹, C. Baranec², N.M. Law³, A.N. Ramaprakash⁴,
S. Tendulkar¹, K. Hogstrom¹, K. Bui¹, M. Burse⁴, P. Chordia⁴,
H. Das⁴, R. Dekany¹, S. Kulkarni¹, S. Punnadi⁴ and R. Smith¹

¹ *California Institute of Technology, 1200 E. California Blvd. MC 11-17,
Pasadena, CA 91125 USA*

² *Institute for Astronomy, The University of Hawaii at Manoa, Hilo, HI
96720 USA*

³ *University of North Carolina at Chapel Hill, Chapel Hill, NC 27599 USA*

⁴ *Inter-University Centre for Astronomy & Astrophysics, Ganeshkhind, Pune,
411007, India*

Received: November 20, 2013; Accepted: January 13, 2014

Abstract. Large surveys, such as the Kepler mission and Palomar Transient Factory, are discovering upwards of thousands of objects which require further characterization at angular resolutions significantly finer than normally allowed by atmospheric seeing. The demands on precious space-based observatories (i.e. Hubble Space Telescope) and large telescopes with adaptive optics (AO) systems (i.e. Keck, VLT, Gemini) leave them generally unavailable for high angular resolution surveys of more than a few hundred targets at a time. To address the gap between scientific objects and available telescopes, we have developed Robo-AO, the first robotic laser AO system, as an economical and efficient imaging instrument for the more readily available 1-3 m class telescopes. The Robo-AO system demonstrates angular resolutions approaching the visible diffraction limit of the Palomar 60-inch telescope. Observations of over 200 stellar objects per night have routinely been performed, with target-to-target observation overheads of less than 1.5 minutes. Scientific programs requiring high-resolution follow-up characterization of several thousands of targets can thus be executed in mere weeks, and Robo-AO has already completed the three largest AO surveys to date.

1. Introduction

Robo-AO is an autonomous laser guide star (LGS) adaptive optics (AO) instrument that robotically operates a telescope, laser, AO system, and science camera to observe several different classes of astronomical objects (Baranec *et al.*, 2013). It is the first system that operates a laser guide star without human oversight. The software architecture for the Robo-AO system has been

designed to be as robust as possible, but also as a system that is simple and flexible to manage and operate. Robo-AO is currently deployed on the 60-inch telescope at Palomar Observatory. Initial science results from the prototype system demonstrate visible-light imaging with angular resolutions approaching the diffraction limit of a 1.5 m telescope ($\approx 0.12''$). Robotic software automations keep target-to-target observing overheads of less than 1.5 minutes (including slew time) leading to the observation of about 20 targets per hour (Riddle *et al.*, 2012), and the completion of the three largest AO surveys to date. Many other implementations of Robo-AO are in various stages of development.

2. System Hardware

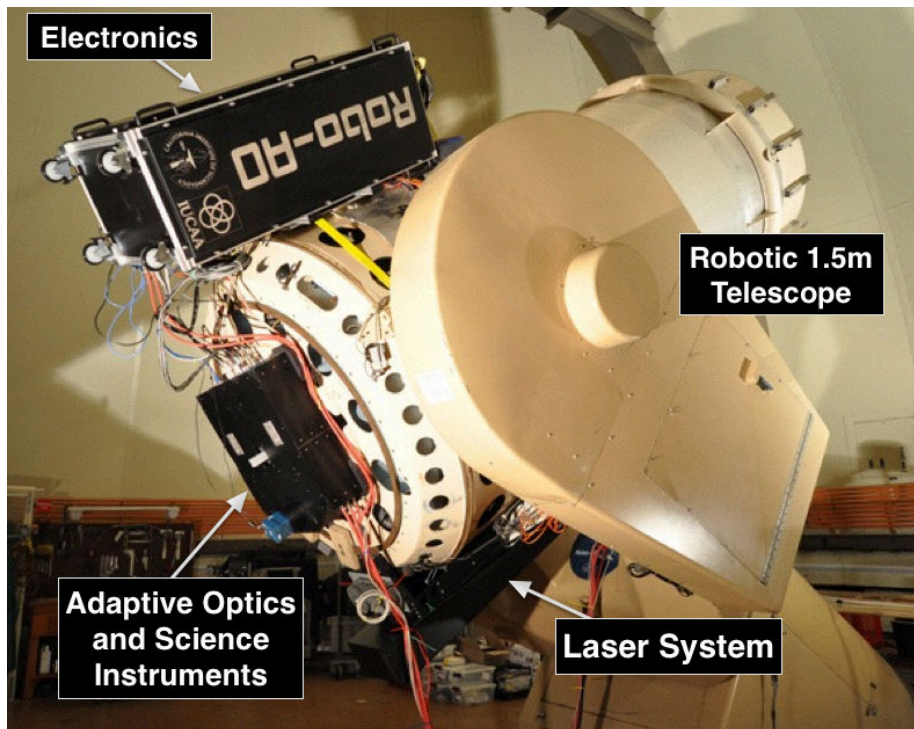


Figure 1. Robo-AO is installed on the Palomar Observatory 60-inch telescope. The adaptive optics and science instruments are installed at the Cassegrain focus, and the laser system and support electronics are attached to opposite sides of the telescope tube for balance.

The Robo-AO instrument was installed on the Palomar Observatory 60-inch (1.5 m) telescope in 2011 for initial testing, with first science and robotic operations occurring in the summer of 2012 (Figure 1). The P60 is a fully automated telescope, which allows remote control through a TCP/IP based command system, and includes a fully automated weather monitoring system to ensure telescope safety during operations (Cenko *et al.*, 2006). The Robo-AO instrument is composed of three structures: the LGS system, the Cassegrain instrument (which includes the AO system, science instruments, and associated hardware), and the support electronics rack.

The core of the Robo-AO LGS system is a pulsed 10-W ultraviolet (355nm) laser (JDSU Q301-HD) mounted in an enclosed projector assembly on the side of the P60 telescope. The laser is focused to a line-of-sight distance of 10 km. Within the adaptive-optics instrument, a high-speed β -BaB2O4 Pockels cell optical shutter (FastPulse Lasermetrics) is used to transmit laser light only returning from a \sim 400 m slice of the atmosphere around the 10 km projector focus (which creates a \sim 2 cm diameter spot in the sky). The ultraviolet laser has the additional benefit of being invisible to the human eye; it is unable to flash-blind pilots, eliminating the need for human spotters located on site as normally required by the Federal Aviation Authority within the U.S.. Unfortunately, the possibility for the laser to damage some satellites in low Earth orbit may exist. For this reason, it is recommended for both safety and liability concerns to coordinate laser activities with an appropriate agency (e.g., with U.S. Strategic Command within the U.S.).

High-order wavefront sensing is performed with an 11×11 Shack-Hartmann wavefront sensor. The detector is an 80×80 pixel format E2V-CCD39 optimized for high quantum efficiency at the laser wavelength (71.9%) and paired with a set of SciMeasure readout electronics. The closed-loop bandwidth of the system is approximately 90-100 Hz. The tip-tilt modes measured in the wavefront sensor are dominated by mechanical vibration and pointing errors. The tip-tilt signal is used to drive the laser systems uplink tip-tilt mirror, thus keeping the Shack-Hartmann pattern centered on the wavefront sensor.

The high-order wavefront corrector within Robo-AO is a MEMS deformable mirror (Boston Micromachines Multi-DM). Robo-AO uses 120 of the 140 actuators to adjust the illuminated surface of the mirror. The actuators have a maximum surface deviation amplitude of $3.5 \mu\text{m}$ which corresponds to optical phase compensation of up to $7 \mu\text{m}$. In typical seeing at Palomar Observatory (median $1.1''$), this compensation length is greater than 5σ of the amplitude of the turbulence induced optical error and therefore results in significant correction headroom. Furthermore, the deformable mirror is used to compensate for static optical errors arising from the instrument and telescope at the cost of reduced dynamic range.

The Robo-AO design uses two science cameras for operation, though only the optical camera is installed in the current system. The visible camera (an Andor iXon3 888 electron-multiplying CCD) has the ability to capture images

with very low electronic (detector) noise, at a frame rate which reduces the intra-exposure image motion to below the diffraction-limited angular resolution. By re-centering and stacking a series of these images, a long-exposure image can be synthesized with minimal noise penalty. The visible camera can also be used to stabilize image tip-tilt motion on the infrared camera; measurements of the position of an imaged astronomical source can be used to continuously command the fast tip-tilt to re-point the image to a desired location.

Individual Robo-AO science observations are currently made using the visible camera with a $44''$ square field of view and $0.043''$ pixel scale. The camera is read out continually at a frame rate of 8.6 Hz during science observations, allowing image motion (which cannot be measured using the laser system) to be removed in software after observations with the presence of a $m_V < 16$ guide star within the field of view. A data reduction pipeline corrects each of the recorded frames for detector bias and flat-fielding effects, automatically measures the location of the guide star in each frame, and then shifts and aligns each frame to achieve an optimal image reconstruction using the Drizzle algorithm (Law *et al.*, 2009). During typical observing, we generally obtain residual wavefront errors in the 160 to 200 nm RMS range, leading to the ability to detect and characterize stellar companions at contrasts of > 5 magnitudes at separations of $0.25-1''$ at visible wavelengths. The large field of view also allows for high-resolution imaging of extended objects. Initial science results demonstrating the capability of Robo-AO have already been published (Law *et al.*, 2012; Muirhead *et al.*, 2013; Swift *et al.*, 2013; Terziev *et al.*, 2013), with many more in preparation.

3. Software Architecture

The Robo-AO robotic control software was developed in parallel with the hardware, to avoid hardware choices that would limit software functionality and to enhance the efficiency of the final system (Riddle *et al.*, 2012). Robo-AO is controlled by a single computer with a Fedora Linux 13 installation for the operating system. The system does not use a real time kernel; this choice was made to save on complication and increase portability of the software. All source code for the Robo-AO project is written in C++; at the time of this writing, the software consists of more than 120,000 lines of documented source code.

The Robo-AO hardware interface software has been developed as a modular system. The software to control each hardware subsystem was developed as a set of individual modules; small standalone test programs have been created to test each of the hardware interfaces. The Robo-AO hardware subsystems are controlled by several software subsystems. These subsystems are run as daemons in the operating system; each separately manages the hardware under its control and runs a status monitor to sample subsystem performance and register errors that occur. Each of the subsystems is composed of many separate functions that initialize the hardware, monitor its function and manage the

operation of the hardware to achieve successful scientific output. In essence, each of the subsystem daemons are individual robotic programs that manage their associated hardware and operate according to external commands.

Each daemon is able to manage operation of its associated hardware automatically and react internally to hardware errors. Communications between the daemons use custom functions for command and control operations that pass continual status information and will automatically restart any daemons that lock up or crash. The daemons are controlled by a central robotic control daemon that commands observation sequences, monitors the state and health of the subsystems, reacts to errors found by the subsystems, and manages all aspects of operation of the observing system. The modular design isolates problems, so that even major issues like daemon crashes result in procedural steps to resume normal operations (instead of system crashes and lost hours of operation), which creates a robust, efficient automated system that can successfully complete scientific observations throughout the night.

A web monitoring interface is available, using PHP for the basic structure, with other software (for making plots or parsing data) using Javascript. Although Robo-AO is a fully automated robotic instrument, it can be operated manually through a text interface if necessary (e.g. for testing purposes). For a thorough description of the operation of Robo-AO, see Baranec *et al.*, (2013).

4. Robo-AO Automated Operations

As a fully autonomous laser AO instrument, Robo-AO executes tasks that are generally performed manually. The robotic system operates multiple subsystems in parallel in order to increase efficiency; for example, to start an observation, the central robotic control daemon will point the telescope, move the science filter wheel, and configure the science camera, laser, and AO system, all before the telescope has settled onto a new science target. The automated laser acquisition process begins once the telescope has completed pointing at the new object. A spiral search algorithm automatically acquires the laser by moving the uplink steering mirror until 80% of the wavefront sensor subapertures have met a flux threshold of 75% of the typical laser return flux. A safety system manages laser propagation onto the sky, and stops laser operations if any errors occur.

Robo-AO uses a newly developed automated system for laser deconfliction that opens the entire area above 50 degrees zenith distance for observation by requesting predictive avoidance authorization for ~ 700 individual fixed azimuth and elevation boxes of ~ 6 square degrees every night. Areas of the sky below 50 degrees zenith distance can be observed as well if scientifically necessary; science observations as low as 65 degrees have been successfully completed. This gives Robo-AO the capability to undertake laser observations of any target overhead at almost any time, increasing observing efficiency by removing the need to preselect targets of observation. It should be noted that this method can

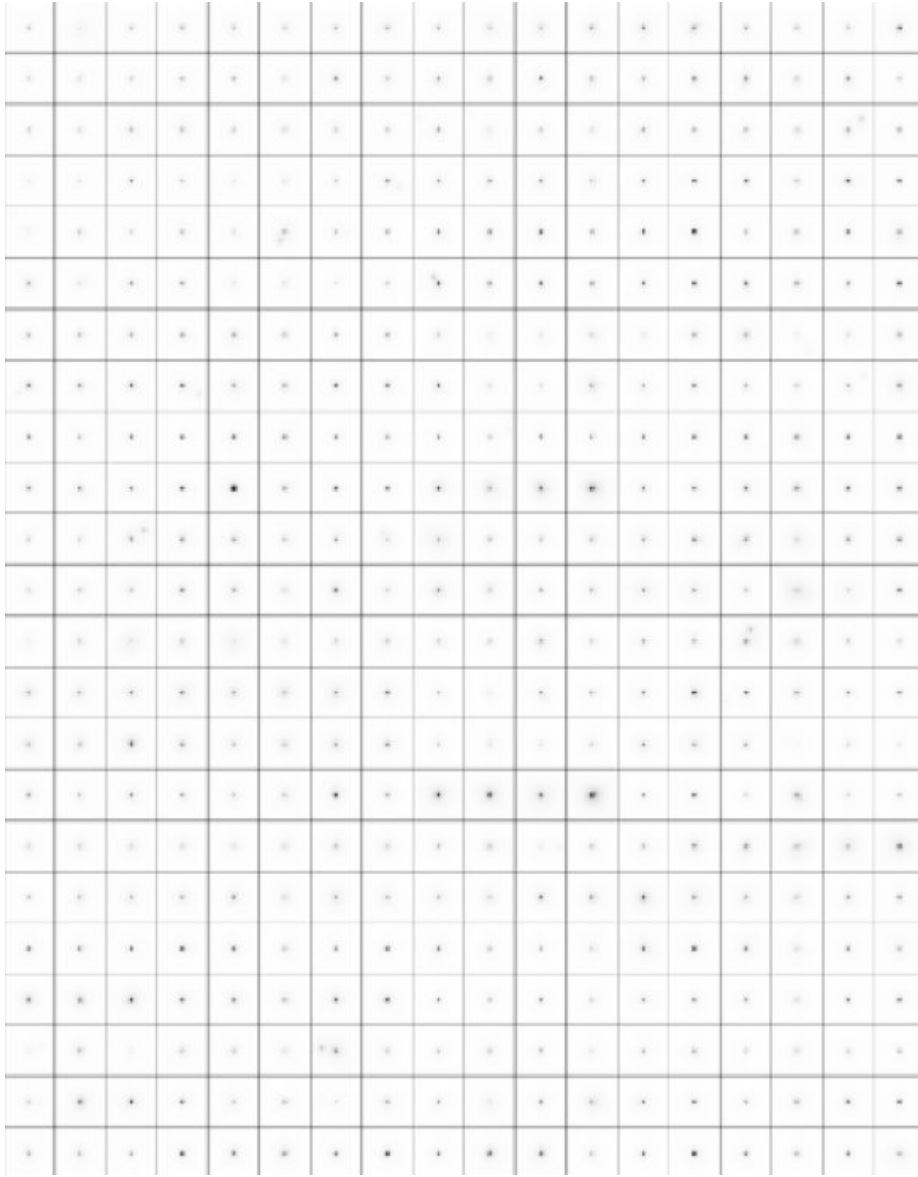


Figure 2. Robo-AO adaptive optics images of 414 stars, executed in just 2.5 nights, as part of the Binarity of the solar neighborhood project (Table 1). Each square represents a $3'' \times 3''$ area, and 90 s of integration in i-band ($\lambda = 765$ nm), sufficient to reach the photon noise floor in the halo and detect companions at $\Delta m \approx 5$ within $0.2''$.

Survey	Instrument	Method	Targets	Time
Binarity of the solar neighborhood [1]	P60 (Robo-AO)	LGS AO	3,081	172 hours
Solar-type dwarf multiplicity [2]	P60 (Robo-AO)	LGS AO	1,115	49 hours
M-Dwarf multiplicity [3]	Calar Alto 2.2-m (AstraLux), NTT (AstraLux)	Lucky	761	300 hours
Washington Double Star Catalog [4]	SOAR (HRCam)	Speckle, AO+Speckle	639	16 nights
Young Solar analogs [5]	KeckII (NIRC2), Hale (PHARO)	NGS AO	266	47 nights
Planets around low-mass stars [6, 7]	KeckII (NIRC2), Subaru (HiCIAO)	NGS AO	125	12 nights
Gemini deep planet survey [8]	GeminiN (NIRI)	NGS AO	85	84 hours (w.o. overheads)
Multiplicity at the bottom of the IMF [9]	KeckII (NIRC2)	LGS AO	78	10 nights
Kepler KOI validation [10]	P60 (Robo-AO)	LGS AO	1,800	112 hours
Kepler KOI validation [11]	MMT (Aries), Hale (PHARO)	NGS AO	90	12 nights
Kepler KOI validation [12]	Calar Alto 2.2-m (AstraLux)	Lucky	98	19 nights

Table 1. A representative sample of the largest ground-based diffraction-limited surveys performed with telescopes greater than 1 m in diameter. References are: [1] Law *et al.* (2014b); [2] Riddle *et al.* (2014); [3] Janson *et al.* (2012); [4] Hartkopf *et al.* (2012); [5] Metchev, Hillenbrand, (2009); [6] Bowler *et al.* (2012); [7] Bowler *et al.* (2014); [8] Lafrenière *et al.* (2007); [9] Kraus, Hillenbrand (2012); [10] Law, *et al.* (2014a); [11] Adams *et al.* (2012); [12] Lillo-Box *et al.* (2012).

be implemented for all laser AO observatories to reduce bookkeeping and make immediate target of opportunity observations possible. A fully automated queue system was developed for Robo-AO that integrates the laser predictive avoidance authorization into the decision making process for which science object to observe next (Hoggstrom *et al.*, 2014). This queue ensures that only objects that are cleared for lasing will be observed at all times, so no time is wasted going to an object that will require laser shutdown during a science observation.

While manually operated laser AO systems typically require 5-35 minutes to prepare for AO operation (Minowa *et al.*, 2012; Neichel *et al.*, 2012; Wizinowich

et al., 2006), Robo-AO requires ~ 50 -60 seconds, on average, from the end of a telescope slew to the beginning of integration with the science camera; many nights of 200+ observations have already been achieved (with a current record of 240). As of this writing, Robo-AO has completed ~ 479 hours of fully robotic operations during 83 nights of allocated telescope time, of which ~ 261 hours (54%) were open-shutter science observing time. In total, almost 10,000 observations were made, with typical exposure times ranging from 30 s to 3 minutes each, which comprise some of the largest high-angular resolution surveys ever performed, as indicated in Table 1. The Robo-AO Binarity of the solar neighborhood survey is a comprehensive study of the companions of nearby stars (< 35 pc) exploring the variation in their properties with stellar mass, metallicity, age and formation/multiplicity environment. The more than 3,000 observed targets are five times larger in number than any other non-Robo-AO adaptive optics survey to date (Figure 2). Robo-AO is able to complete these large surveys much faster than other AO systems, such as having observed ten times the number of Kepler Objects of Interest (KOI) than larger telescope facilities in half of the observing time.

5. The Future of Robo-AO

The Robo-AO collaboration is currently in the process of constructing a low-noise wide-field imager using a $2.5 \mu\text{m}$ cutoff Teledyne HAWAII-2RGTM detector which was delivered to Caltech in September 2012. The Robo-AO instrument has an IR camera port designed to accommodate the expected 70-kg mass of the infrared camera. As part of our integration plan, we will develop automated routines for configuring the high-speed infrared tip-tilt sensing and recording of infrared science data in much the same way as has been done with the visible Robo-AO camera, and then integrate the IR camera into the automation and queue system software. Special procedures for dealing with infrared data, including taking sky-flats, backgrounds, and darks, as well as compensating for nonlinear responses and amplifier glow, will be developed and included as part of a standard data pipeline.

A clone of the current Robo-AO system is currently being developed for the 2-m IUCAA Girawali Observatory telescope in Maharashtra, India (Gupta *et al.*, 2002). Adaptations in optical prescriptions have been made to accommodate the slightly different F/#, F/10 vs. F/8.75, different mounting interface and telescope interface software. No other major changes are anticipated - minimizing further development and control costs. The system is expected to see first light in 2014. In addition to this clone, Pomona College has used the Robo-AO design and software to develop an AO instrument, built mainly by undergraduate students, that has already achieved on-sky AO correction (Severson *et al.*, 2013), and the Minerva project is basing their robotic control software on the Robo-AO system (Hoggstrom *et al.*, 2013). The modular design of Robo-AO

and the relative simplicity of the instrument make it straightforward to replicate or adapt the system to other observatories and instruments.

The prototype Robo-AO at Palomar has been crucial in validating the current sample of KOIs, having observed over three-quarters of the 2,036 host stars (from the January 2013 release). A complementary follow-on mission to Kepler is the Transiting Exoplanet Survey Satellite (TESS). TESS will execute a shallower survey compared to Kepler, with the majority of objects $m_V < 16$, but over the entire sky. It is estimated that there may be as many as ten or more times as many transit signals discovered by TESS during its mission lifetime which could all be validated by Robo-AO in less than a year. To make this happen, we are planning to deploy such systems at either or both of the 2.2 m UH and 3 m IRTF telescopes on Mauna Kea and are looking for partners for a facility-class Robo-AO in the southern hemisphere. Eventually, a network of globally linked Robo-AO systems could observe the night sky at high resolution operating as one unified robotic instrument (Riddle, 2011).

The next generation large telescopes all will require an automation of tasks of the same order of magnitude as the Robo-AO robotic system in order to achieve their operational requirements (Ellerbroek *et al.*, 2010). The lessons learned from developing and operating Robo-AO can inform the process of developing the next generation of astronomical instruments.

Acknowledgements.

The Robo-AO project is supported by collaborating partner institutions, the California Institute of Technology and the Inter-University Centre for Astronomy and Astrophysics, by the National Science Foundation under Grant Numbers AST-0906060 and AST-0960343, by a grant from the Mt. Cuba Foundation, by the Office of Naval Research under grant N00014-11-1-0903, and by a gift from Samuel Oschin. We are grateful for the continued support of the Palomar Observatory staff for their ongoing support of Robo-AO on the 60-inch telescope, particularly S. Kunsman, M. Doyle, J. Henning, R. Walters, G. Van Idsinga, B. Baker, K. Dunscombe and D. Roderick.

References

- E. R. Adams, *et al.*: 2012, *ApJ* **144**, 42
- C. Baranec, *et al.*: 2013, *J. Vis. Exp.* **72**, e50021, doi:10.3791/50021
- B. P. Bowler, *et al.*: 2012, *ApJ* **753**, 142
- B. P. Bowler, *et al.*: 2014, in preparation
- S. B. Cenko, *et al.*: 2006, *PASP* **118**, 1396-1406
- B. Ellerbroek, *et al.*: 2010, *Proceedings of the SPIE* **7736**, 14
- R. Gupta, *et al.*: 2002, *Bulletin of the Astronomical Society of India* **30**, 785
- W. I. Hartkopf, A. Tokovinin and B. D. Mason: 2012, *ApJ* **143**, 42
- K. Hoggstrom, *et al.*: 2014, in preparation
- M. Janson, *et al.*: 2012, *ApJ* **754**, 44
- A. L. Kraus and L. A. Hillenbrand: 2012, *ApJ* **757**, 141
- D. Lafrenière, *et al.*: 2007, *ApJ* **670**, 1367-1390

- N. M. Law, *et al.*: 2009, *ApJ* **692**, 924-930
N. M. Law, *et al.*: 2012, *ApJ* **757**, 133
N. M. Law, *et al.*: 2014a, in preparation
N. M. Law, *et al.*: 2014b, in preparation
J. Lillo-Box, D. Barrado and H. Bouy: 2012, *A&A* **546**, A10
S. Metchev and L. A. Hillenbrand: 2009, *ApJS* **181**, 62-109
Y. Minowa, *et al.*: 2012, *SPIE Adaptive Optics Systems III* **8447**, 8447-52
P. Muirhead, *et al.*: 2013, *ApJ* **767**, 111
B. Neichel, *et al.*: 2012, *SPIE Adaptive Optics Systems III* **8447**, 8447-176
R. Riddle: 2011, *IUSSTF Workshop on Astronomy with Adaptive Optics on Moderate-sized Telescopes*, Pune, India
R. Riddle, *et al.*: 2012, *SPIE Adaptive Optics Systems III* **8447**, 8447-96
R. Riddle, *et al.*: 2014, in preparation
S. Severson, *et al.*: 2013, *SPIE MEMS Adaptive Optics VII* **8617**, 8617-09
J. Swift, *et al.*: 2013, *ApJ* **764**, 105
E. Terziev, *et al.*: 2013, *ApJS* **206**, 18
P. Wizinowich, *et al.*: 2006, *PASP* **118**, 297-309